P-13-49

Forsmark

Measurements of electrical potential gradients in the Forsmark area autumn 2013

Laust B Pedersen, Chunling Shan, Lars Dynesius
Uppsala University

November 2013

Svensk Kärnbränslehantering AB
Swedish Nuclear Fuel
and Waste Management Co

Box 250, SE-101 24 Stockholm
Phone +46 8 459 84 00

ISSN 1651-4416
SKB P-13-49
ID 1399036

Forsmark

Measurements of electrical potential gradients in the Forsmark area autumn 2013

Laust B Pedersen, Chunling Shan, Lars Dynesius
Uppsala University

November 2013

Keywords: Electrical potentials, boreholes, HVDC

Abstract

The Fenno-Skan 1 and 2 HVDC power transmission link between Finland and Sweden consists of two monopolar circuits. The direction of the current in each of the two cables is always the same irrespective of whether electrical power is exported to or imported from Finland. Normally the two circuits are balanced with approximately the same electrical current, but in opposite direction, in each cable. If one of the cables is out of operation, the Earth replaces one of the cables as the return loop.

The aim of the present study was to quantify the potential gradients in the Forsmark area under varying loads of the Fenno-Skan 1 and 2. During the period 2013-09-23 to 2013-10-09 measurements of the time variations of the electrical potential gradients were conducted in two sets of boreholes each of which consisted of three boreholes. In each setup the electrical potential differences between the respective boreholes were measured in two independent horizontal directions at a depth of approximately 90 m. In addition, the three magnetic field components were monitored at each of the measurement setups in order to study the effect of natural magnetic variations on the electrical potential variations in the boreholes.

Generally the results show a very clear correlation between the variations in the net current in the Fenno-Skan cables and the potential gradients. There are considerable differences between measured potential gradients between the two setups. Part of the variation can be understood as due to the direction from the injection point in Sweden, located at Fågelsundet about 25 km NW of Forsmark, to the measurement locations at Forsmark. Other parts are interpreted to be due to lateral variations in electrical conductivity in the Forsmark area whereby large jumps in the electrical potential can arise if currents are directed parallel to the gradients of the electrical conductivity. Such gradient discontinuities can be caused by transition from salt-water dominated to fresh water dominated regimes in the Earth's crust or as a result of fracture zones that may form a strong conductivity contrast to the surrounding more intact rocks.

In spite of these complications, the average sensitivity of the potential gradients to the current injected at Fågelsundet can be assessed to be in the order of the magnitude 1 mV/m per 1,000 A.

Sammanfattning

HVDC-förbindelsen Fenno-Skan 1 och 2 mellan Finland och Sverige består av två monopolära kretsar. Riktningen för strömmen i var och en av de två kablarna är alltid densamma oberoende av om elkraft exporteras till eller importeras från Finland. Vid normaldrift är de två kretsarna balanserade med ungefär samma, men motsatt riktad ström, i båda kablarna. Om en av dessa är ur drift, går strömmen från den andra kabeln i retur genom jorden.

Syftet med föreliggande studie var att kvantifiera potentialgradienterna i Forsmarksområdet under varierande last på Fenno-Skan 1 och 2. Under perioden 2013-09-23 till 2013-10-09 utfördes mätningar av de tidsliga variationerna av potentialgradienterna på två platser med vardera tre borrhål. På båda platserna mättes de elektriska potentialskillnaderna mellan respektive borrhål i två oberoende horisontella riktningar på ett djup av ungefär 90 m. Dessutom registrerades de tre magnetiska fältkomponenterna på båda platserna för att studera effekten av naturliga magnetiska variationer av de elektriska potentialgradienterna mellan borrhålen.

Generellt visar resultaten en mycket klar korrelation mellan variationer i nettoströmmen genom Fenno-Skan kablarna och uppmätta potentialdifferenser. Det finns dock stora skillnader mellan de uppmätta potentialgradienterna vid de två platserna. En del av skillnaden kan bero på olika riktningar till strömelektroden i Sverige, belägen vid Fågelsundet ca 25 km NV om Forsmark. Övriga skillnader kan bero på laterala variationer i elektrisk konduktivitet i Forsmarksområdet genom att stora hopp i den elektriska potentialen kan uppstå om strömmarna är riktade parallellt med gradienter av den elektriska ledningsförmågan. Sådana diskontinuiteter hos potentialgradienterna kan orsakas av t ex övergången mellan områden med saltvatten och färskvatten i jordskorpan eller uppstå som en följd av sprickzoner med mycket god elektrisk ledningsförmåga jämfört med det omgivande berget.

Trots dessa komplikationer kan den genomsnittliga känsligheten för potentialgradienterna i Forsmarksområdet från strömelektroden vid Fågelsundet bedömas vara av storleksordningen 1 mV/m per 1 000 A.

Contents

1 Introduction

The work was carried out in accordance with the activity plan listed in Table 1-1. The activity plan is an SKB internal controlling document. No method description exists for this type of measurements.

Measurements of potential gradients were performed between the two sets of boreholes HFM34-HFR101-KFR106 localized in the SFR-area and KFM23-KFM21-KFM13 localized in the area of the planned repository for spent fuel. Figure 1-1 shows the localization of the boreholes.

The original results are stored in the primary data base Sicada and are traceable by the activity plan number.

Table 1-1. Controlling documents for performance of the activity.

Activity plan	Number	Version
Jordströmsmätningar i borrhål i Forsmark	AP SFK-10-066	1.1

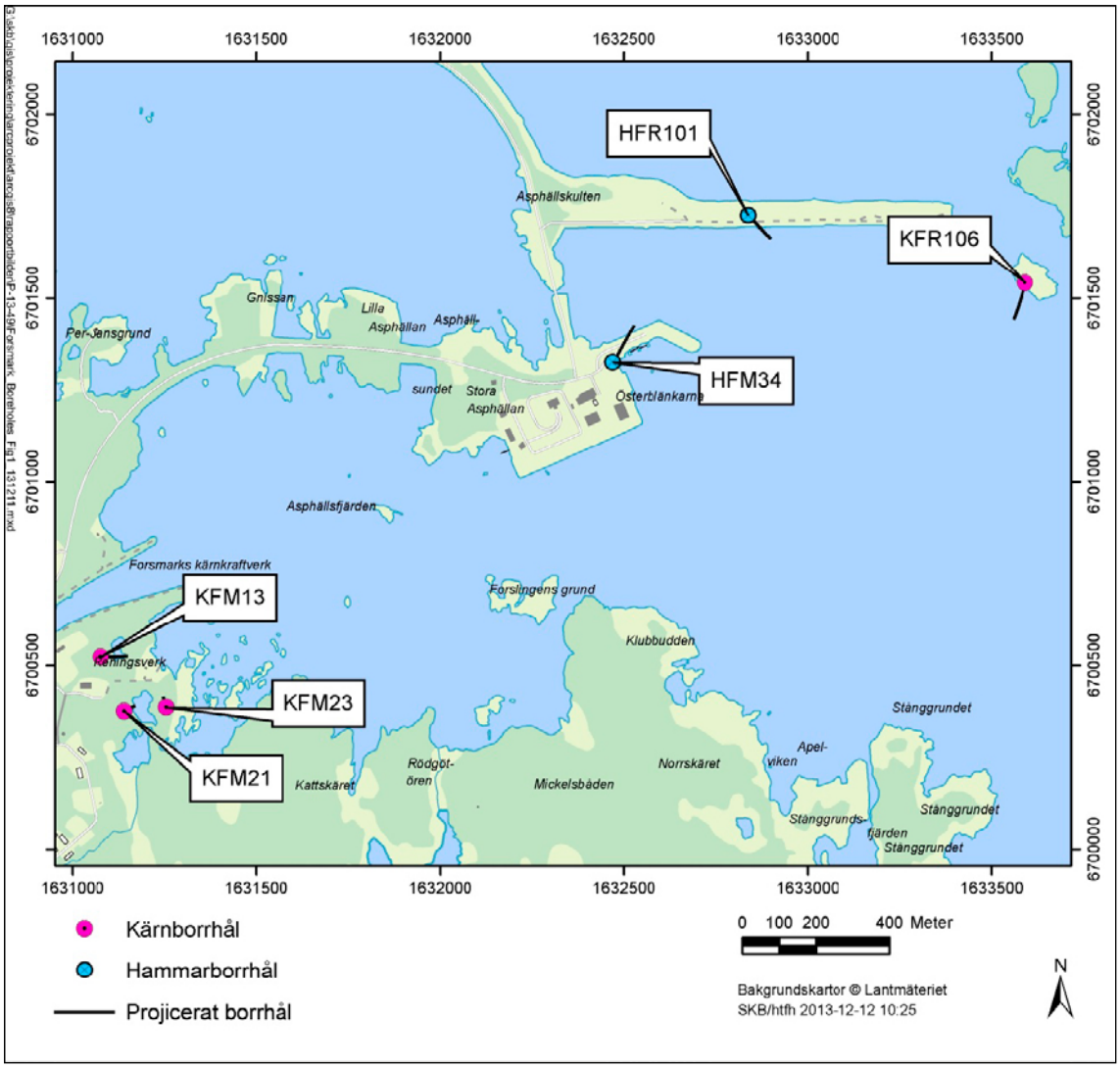

Figure 1-1. *Position of the two sets of boreholes.*

2 Objective and scope

The objective of the present measurements was to investigate if there is a correlation between the potential gradients in the Forsmark area and the net current from the Fenno-Skan electrode station in Fågelsundet and, if so, to describe the character of that correlation.

The Fenno-Skan HVDC link between Sweden and Finland allows for transmission of up to 1,350 MW. Two HVDC cables connect the inverters/converters on the Swedish and Finnish side. The electrode station, common for both cables Fenno-Skan 1 and 2, is localized in Fågelsundet approximately 25 km north of Forsmark. see Figure 2-1. The converter/inverter is connected to the electrode station with an overhead line. A photo of the overhead line is shown in Figure 2-2. The purpose of the overhead line and the electrode station is to carry the difference current between the currents in Fenno-Skan 1 and 2, which can be up to ca 1,000 A.

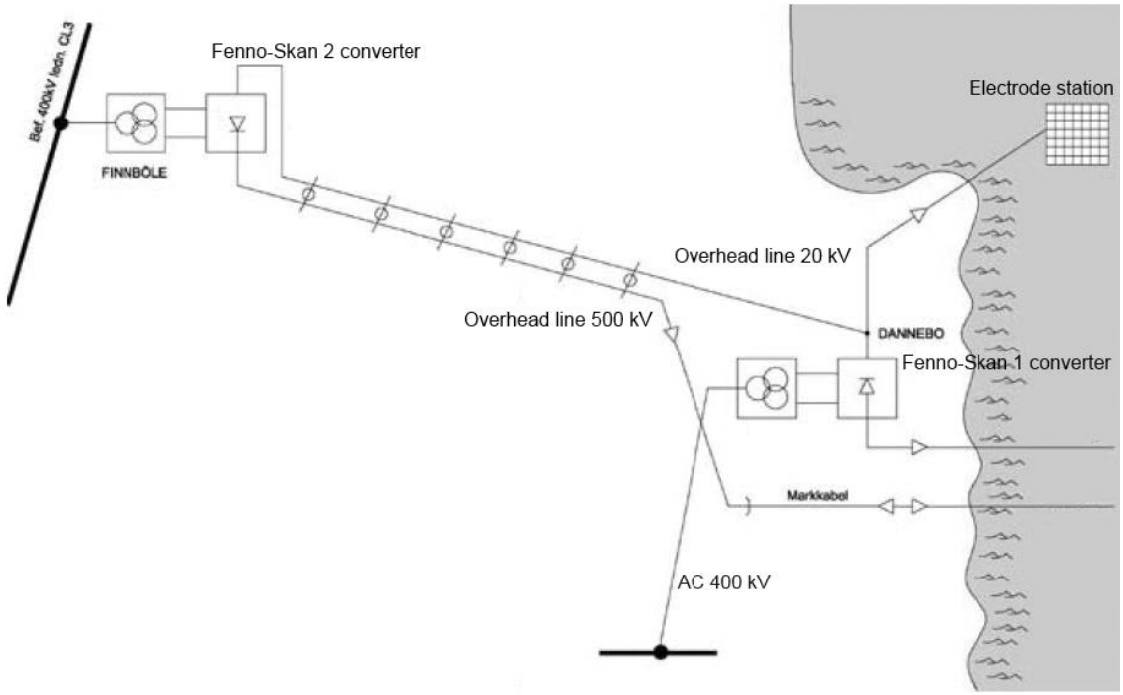

Figure 2-1. *Sketch of the Fenno-Skan 1 and 2 layout. The distance between the two converters are ca 75 km, and the distance from Dannebo to the electrode station is ca 25 km. Figure modified from Svenska Kraftnät, Environmental Impact Assessment (MKB).*

Figure 2-2. *Photo of the DC overhead line between the inverter at Forsmark and the electrode at Fågelsundet. The voltage in the overhead line is of the order of magnitude 2 kV.*

3 Equipment

3.1 Description of equipment/interpretation tools

Two sets of long period MagnetoTelluric (MT) equipment were used. A detailed description of the equipment is given in the paper by Smirnov et al. (2008). The long period instruments use fluxgate magnetometers to cover the period band 30 s – DC. For measuring potential gradients (or electric fields) we use pairs of identical Pb-$PbCl_2$ electrodes. Each instrument is powered by two 90 Ah batteries, which are continuously recharged from 230 V mains. All signals are collected in a central box with signal conditioner, AD converter and data storage devices. For the borehole measurements we use specially designed Pb-$PbCl_2$ electrodes that are directly mounted on special watertight cables. Thus there is no external coupling between electrodes and cables. This makes the measurement system very robust under chemically active conditions that sometimes prevail in boreholes with high mineral content such as salt water. The special cable-electrode connections for the borehole measurements were manufactured by Uppsala University. Photography of the electrodes is shown in Figure 3-1. In addition to special cables purchased by SKB in an earlier project we also purchased extra cables to be able to connect the two sets of boreholes to the data acquisition systems placed in the center of the setup.

Figure 3-1. *Photography of the Pb-$PbCl_2$ electrodes.*

4 Execution

4.1 General

We installed electric sensors in two setups with two sets of boreholes in each setup at a vertical depth of approximately 90 m. In addition we measured the three magnetic field components for each setup. The measurements took place over a period of two weeks during which the Fenno-Skan HVDC powerline was operated with varying current loads in the range –1,500 A to +1,300 A. From an earlier experiment (Pedersen et al. 2008) it is expected that such loads will generate electric fields at Forsmark of the approximate magnitude 1 mV/m per 1,000 A. In this experiment we used two setups separated approximately 2 km. This will enable us to get a more detailed knowledge of how the electric field varies on a small scale, not only in magnitude, but also in direction at the 90 m depth level at Forsmark.

The Fenno-Skan HVDC system connecting Sweden and Finland consists of two cables. Under normal conditions the current in the two cables is balanced, implying no net current to be injected in the electrode at Fågelsundet.

The Fenno-Skan 1 cable carries positive currents towards Fågelsundet in Sweden while the Fenno-Skan 2 cable carries positive current towards Finland. It should be noted that the direction of current flow is always the same in the two cables irrespective of whether power is delivered to Finland or to Sweden. In case one of the cables is out of function, the return current flows through the crust and sea water and hence generate substantial electric fields (or voltage differences) to large distances away from the grounding points. In this report we describe how the electric and magnetic fields change when the differential current in the cables deviates from zero, whereby some of the current is fed into the Earth.

4.2 Execution of field work

The analogue signals from the electromagnetic sensors are connected directly to a 24 bits data logger with GPS timing. We used two separate data loggers (each containing six channels) that were accurately synchronised using GPS clocks. One full five component measurement corresponding to borehole measurements of the horizontal electric and three component surface magnetic fields were recorded on one logger. The grounding electrodes for each setup were put in wet places, of which one was by the small lake and the other (on the pier) was in seawater.

All magnetic sensors were carefully buried to reduce as much as possible of artificial signals from wind noise and daily temperature variations. The two MT systems were running for about 2 weeks, and no malfunctioning was detected at this stage, except that one grounding electrode was in bad contact with the ground because of a drop in groundwater level. However, this had no influence on the stability of the measurements.

After the field work was finished and the first results had emerged from data processing, the question arose as to whether our electrode system was subject to self-potentials and/or if the electronic system had a considerable DC bias. We therefore conducted several experiments in the laboratory. All electrodes were tested for self-potentials by submerging them in pairs into the same bucket with water; and only minute self-potentials could be identified. Similarly, we short-circuited the input terminals of our system in order to control for DC off-set, but only negligible off-sets could be identified. We therefore can conclude that measured DC components at Forsmark must be due to real DC phenomena related to the flow of electric currents.

4.3 Data handling/post processing

The original digital data stored in the data logger were represented by 24 bits with the lowest bit corresponding to 1 μV referred to input. The two channels recording the electric field variations are converted into units of mV/m by dividing with the dipole lengths for each of the two borehole arms, representing the distance between the electrodes at a depth of approximately 100 m in the two boreholes. The three magnetic field channels are converted into units of nT considering the sensitivity of the sensors as 1.33 nT/mV.

The time series of the electric and magnetic fields are plotted as a function of time. They are compared with the amplitude of the injection currents from the same time.

The fields are averaged over one hour intervals to make them compatible with the average current injected at Fågelsundet. A regression study was carried out by considering the fields and currents as variables and assuming that their relationship is linear. Linear regression consists of finding the best-fitting straight line through the points. The slope of the best-fitting line, also shows how incremental changes of the current at Fågelsundet affect incremental changes in the measured electric and magnetic fields at Forsmark. In this case with 6 borehole pairs and 6 magnetic field components from the two central sites for each setup we show 12 such regression plots.

We estimate the direction of the electric field line at Forsmark assuming that Earth can be treated as a layered half-space. Under this condition the electric field will approximately be directed along the line connecting the measurement positions and the grounding point at Fågelsundet, because the grounding point in Finland is located sufficiently far away in order to have very little influence on the direction of the field at Forsmark. We denote this direction as the tangent direction, t, and the direction normal to it as the normal direction, n. We decompose the measured electric fields into the t–n coordinate system in order to see more clearly how local conductors and resistors distort the electric fields with respect to amplitude as well as to direction. An attempt was made to estimate magnetotelluric transfer functions (to study the deep electrical properties under Forsmark) in time intervals where the injected current at Fågelsundet vanishes. However, the two measuring sites are too noisy and it is clear that most of the electromagnetic signals recorded at Forsmark are due to a combination of the DC current at Fågelsundet and man-made noise generated in the Forsmark area.

4.4 Analyses and interpretations

The plots of the original time-series of electrical potential differences (electric fields) and the three components of the magnetic fields already clearly show how injected currents at Fågelsundet generate electromagnetic fields at Forsmark at a depth of approximately 100 m below the surface. A regression analysis further illustrates the linearity between the two, but it also illustrates that there are clear deviations from linearity at certain time intervals, indicating that the electrical conditions at Forsmark are more complicated than initially anticipated.

4.5 Nonconformities

We report no nonconformities.

5 Results

5.1 The SFR site

We first present the results from the setup on the pier described by the two vectors V1 and V2 in Table 5-1 and specified more detailed in Table 5-2. The two vectors are nearly orthogonal so that the corresponding time series carry independent information as seen on the map in Figure 5-1.

We first show the magnetic field variations from the Fiby Magnetic Observatory at Uppsala in Figure 5-2. We notice that the variations of the natural magnetic field during the measurement period are small with amplitudes around 20 nT except for the period between October 1 and 2, where amplitudes reach around 300 nT. Under simplified assumptions of a homogeneous half-space of resistivity 3,000 Ohm/m, and for a period of 3,000 s, the corresponding horizontal electric field will be of the order 400 mV/km. Compared with the real measurements at the pier site shown in Figure 5-3, this seems to give a reasonable estimate of the electric field amplitudes during a moderate electric storm with mean period around 3,000 s. We notice that this is similar in amplitude to the field generated by a 1,000 A current injection at Fågelsundet.

Looking closer at the electric field variations in Figure 5-3 it is noticed that the electric field in the x-direction (V1) exhibits a peculiar behaviour when no current is injected at Fågelsundet. On September 28 the field suddenly jumps 0.2 mV/m even though no current is injected at Fågelsundet. After about 12 hours the field jumps back to its normal value. A similar strange behaviour is observed during the last three days of the recording period. The field exhibits two jumps and a slow decay in the absence of injected current at Fågelsundet. In contrast to the x-component of the electric field the y-component follows nicely the course of the injected current.

We performed a regression analysis between the input current at Fågelsundet (representing a one hour average) and all five electromagnetic components (averaged over one hour) measured on the SFR site. Here we only show the regression analysis for the two horizontal electric fields in Figure 5-4. The remaining fields and corresponding regression analyses are shown in Appendix 1.

The deviation from linear behaviour is most clearly seen on E_x. However, the slope is hardly affected by these deviations, whereas the intercept is strongly affected. We neglect the upward shift of the curve for E_x and calculate the intercept by visual inspection. The slopes along V1 and V2 are estimated at –0.25 mV/km/A and –0.43 mV/km/A, respectively, and the intercepts are close to zero for both directions, 0.07 and –0.06 mV/m (70 mV/km and –60 mV/km) respectively.

We show all results for the electric field in the fixed coordinate system *t–n* where *t* is directed from Fågelsundet to Forsmark while *n* is rotated clockwise by 90 degrees with respect to *t*. For this station *t* has an azimuth of 143 degrees from N to E and *n* an azimuth of 233 degrees from N to E. In the *t–n* coordinate system the expected component along *n* should be small if a layered half-space model of the Earth crust is applicable. With reference to Appendix 3 we calculate the slopes in the *t* and *n* directions as –0.32 mV/km/A and +0.27 mV/km/A, respectively, indicating that the distribution of electric conductivity (resistivity) in the Forsmark area is highly complex, giving rise to amplification/reduction as well as rotation of the electric field from the injected current at Fågelsundet. Adding the two slopes vectorially gives an effective slope of 423 mV/km/kA and an azimuth of 283°.

Table 5-1. Distance and direction between the electrode positions in the boreholes.

		Electrode separation	Direction
V1	HFM34 – HFR101	491 m	48.3°
V2	HFR101 – KFR106	744 m	104.7°

Table 5-2. Borehole parameters and calculated length for the positioning of the electrodes to achieve an approximate depth of about 87 m. Coordinates are in RT90 2.5 gon V 0:-15, RHB 70.

Bh Id	Bh inclination	Electrode position at borehole length	Elevation (RHB 70)	Coordinates at electrode position	Rock types and nearby deformation zones
HFR101	–70°	96 m	–86.35 m	6701699 N 1632864 E	Pegmatitic granite. Deformation zone at 101–115 m.
HFM34	–56°	105 m	–86.74 m	6701373 N 1632498 E	Pegmatitic granite. Deformation zone (Singö zone) at 37–133 m.
KFR106	–70°	94.5 m	–87.65 m	6701510 N 1633583 E	Metagranite-granodiorite. Deformation zones at 86 m och 100.5 m.

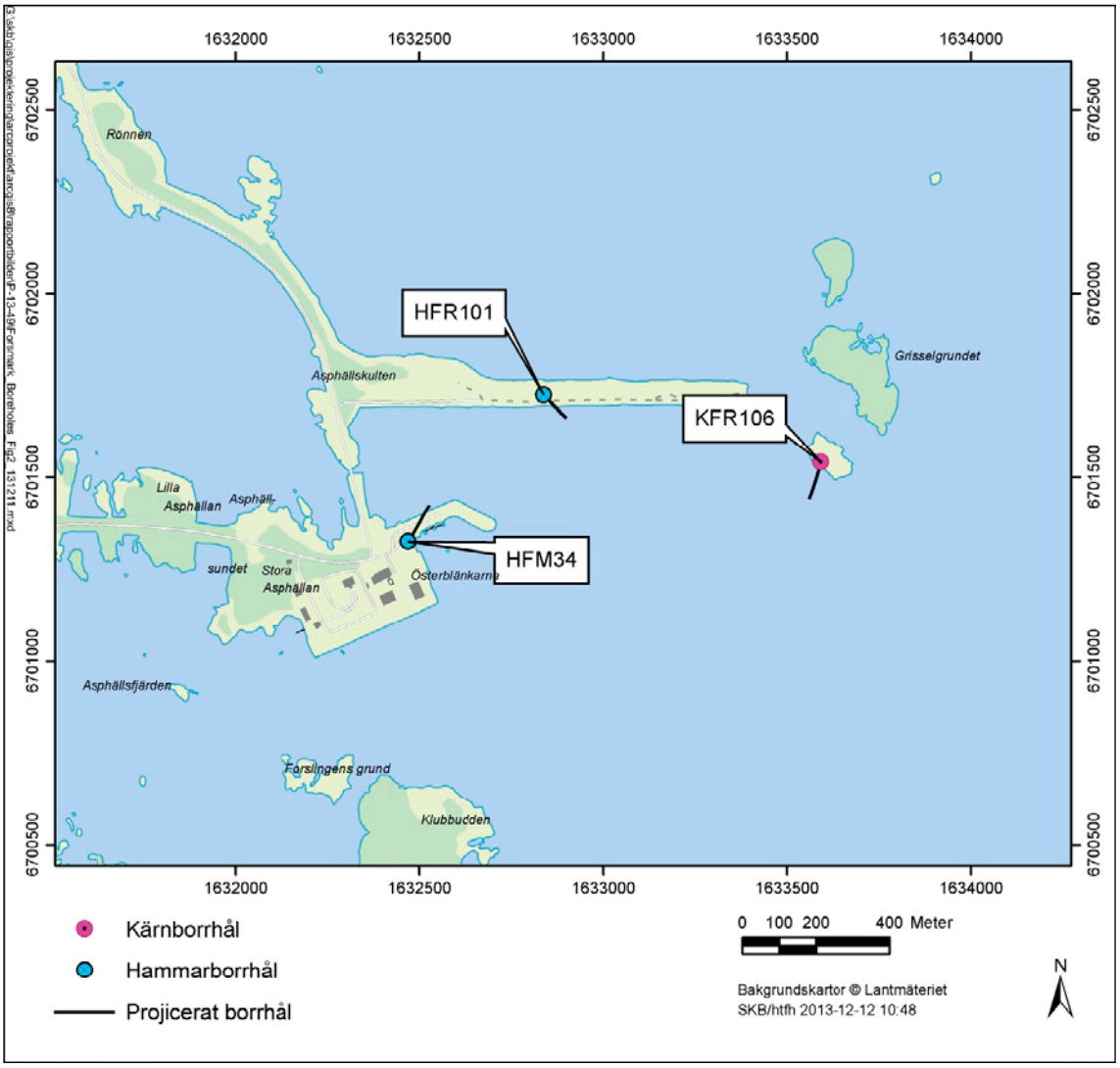

Figure 5-1. *Boreholes at SFR with the boreholes HFR101, FHM34 and KFR106 marked together with the vectors V1 and V2.*

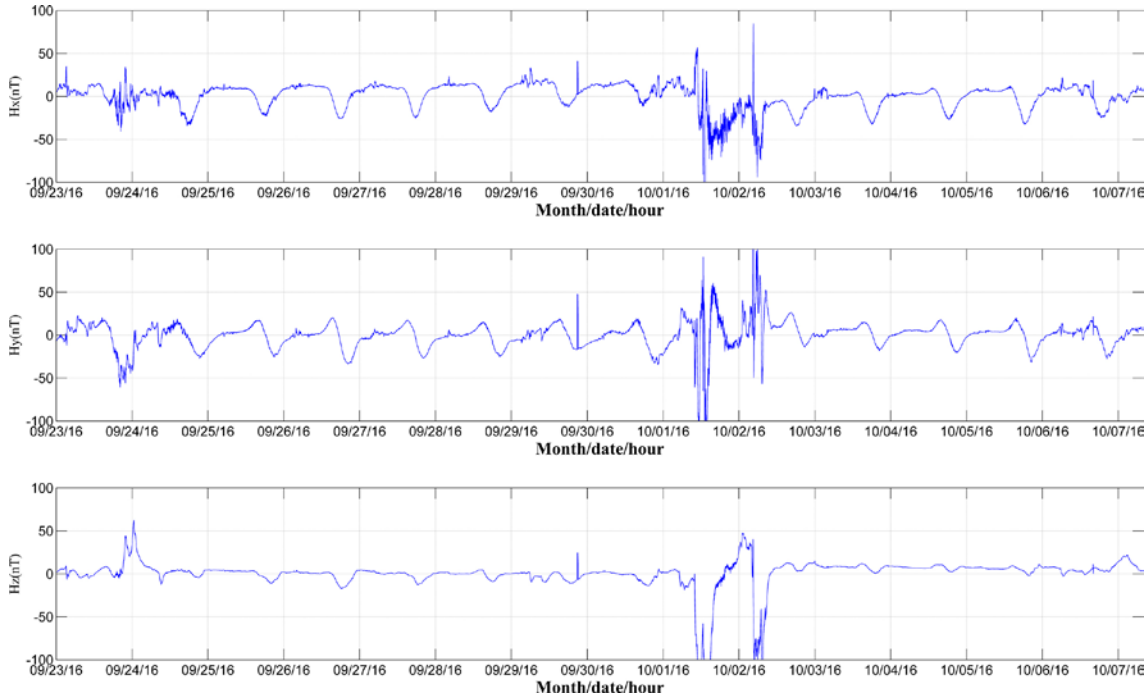

Figure 5-2. *Variation of the three orthogonal magnetic field components at Fiby Observatory, Uppland.*

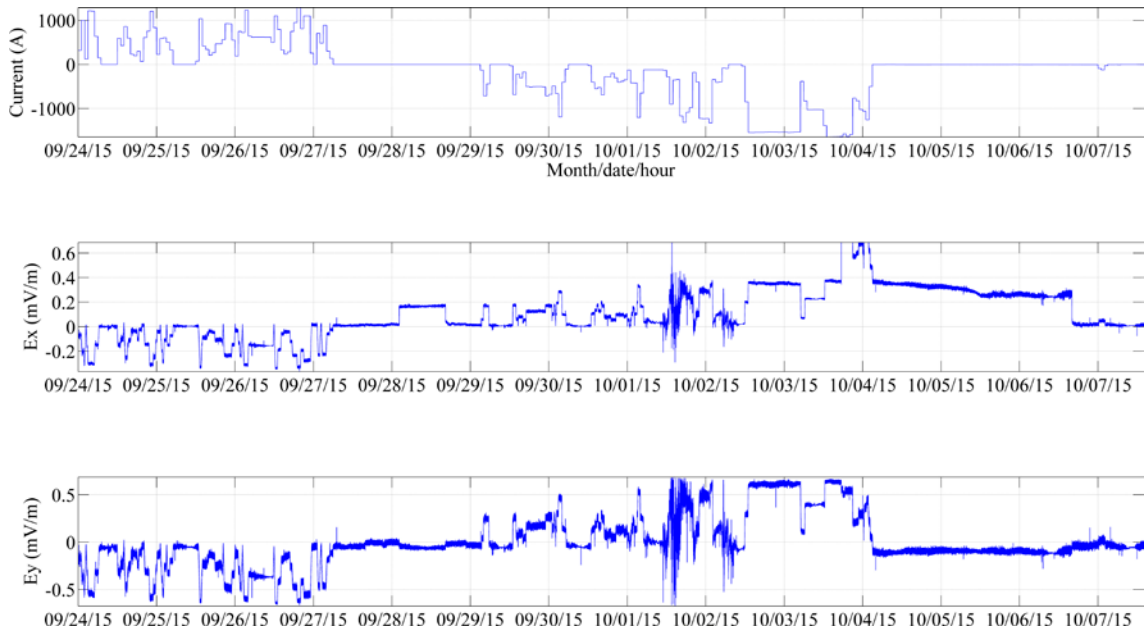

Figure 5-3. *Variation of the horizontal electric field at the SFR site, Forsmark, (lower diagrams), and current injected at Fågelsundet (upper diagram). Ex corresponds to V1 and Ey to V2.*

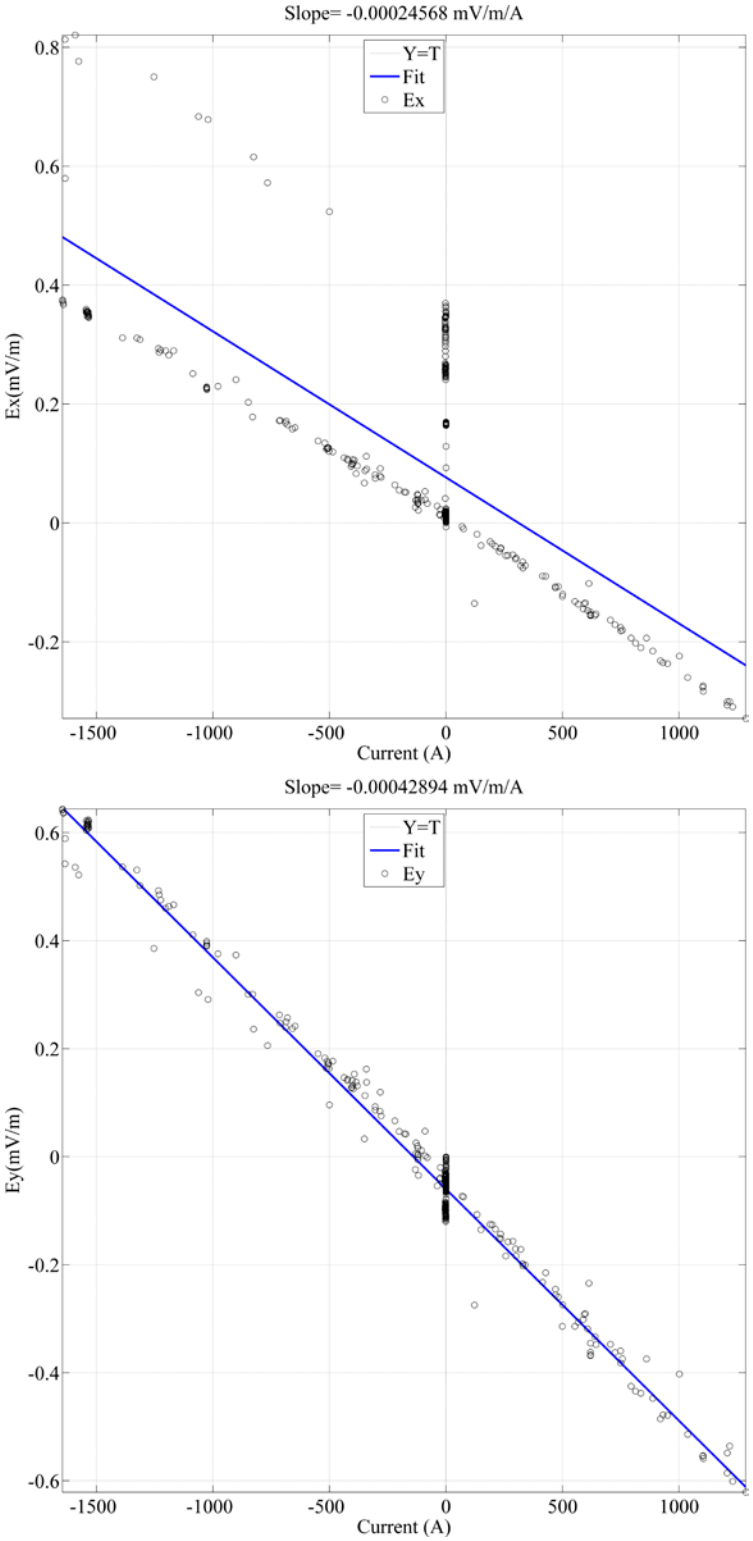

Figure 5-4. *Regression analysis of measured electric fields, Ex (V1) and Ey (V2), on the pier site.*

5.2 The land site

Next we present the results from the setup on the land site described by the two vectors V3 and V4 in Table 5-3 and specified more detailed in Table 5-4. The two vectors are nearly orthogonal so that the corresponding time series carry independent information as seen on the map in Figure 5-5.

Looking closer at the electric field variations in Figure 5-6 it is noticed that the electric components in both x- (V3) and y- (V4) directions are non-zero when no current is injected at Fågelsundet. This bias can be read off the regression lines shown in Figure 5-7 to be equal to +0.32 mV/m and –1.65 mV/m, respectively. These DC components in the electric field components are much larger than those observed at the pier site.

The regression analysis between the input current at Fågelsundet (representing a one hour average) and all five electromagnetic components (averaged over one hour) measured at the land site are shown in Figure 5-7 for the horizontal electric components and in Appendix 2 for the remaining components.

For this site there is no obvious deviation from linear behavior between the current injected and the two horizontal electric field components. The slopes along V3 and V4 are estimated at +0.37 mV/km/A and –2.01 mV/km/A, respectively. Thus along V4 both the bias and slope are much larger than for any of the other three directions measured.

We show all results for the electric field in the fixed coordinate system *t–n* where *t* is directed from Fågelsundet to Forsmark while *n* is rotated clockwise by 90 degrees with respect to *t*. For this station *t* has an azimuth of 147 degrees from N to E and *n* an azimuth of 237 degrees from N to E. In the *t–n* coordinate system the expected component along *n* should be small if a layered half-space model of the Earth crust is applicable. With reference to Appendix 3 we calculate the slopes in the *t* and *n* directions as –0.89 mV/km/A and +1.65 mV/km/A, respectively, indicating once again that the distribution of electric conductivity (resistivity) in the Forsmark area is highly complex, giving rise to both amplification/reduction and rotation of the electric field from the injected current at Fågelsundet. Adding the two slopes vectorially gives an effective slope of 2,040 mV/km/kA and an azimuth of 262.9°.

Table 5-3. Distance and direction between the electrode positions in the boreholes.

		Electrode distance	Direction
V3	KFM21 – KFM13	139 m	–16.8°
V4	KFM21 – KFM23	78 m	73.5°

Table 5-4. Borehole parameters and calculated borehole length for the positioning of the electrodes to achieve an approximate depth of about 90 m. Coordinates are in RT90 2.5 gon V 0:-15, RHB 70.

Bh Id	Bh inclination	Electrode position at borehole length	Elevation (RHB 70)	Horizontal coordinates at electrode position	Rocktypes and close by fractures at electrode positions
KFM13	–61°	109.5 m	–92.5 m	6700525 N 1631133 E	Metagranite-granodiorite. Cross zone at 81.72–81.78 m. A breccia at 145.50–145.57 m.
KFM21	–70°	101 m	–92.5 m	6700393 N 1631173 E	Metagranite-granodiorite. Cross zone at 66.30–66.38 m.
KFM23	–73°	99 m	–92.4 m	6700415 N 1631248 E	Metagranite-granodiorite. Cross zone at 82.74–82.78 m.

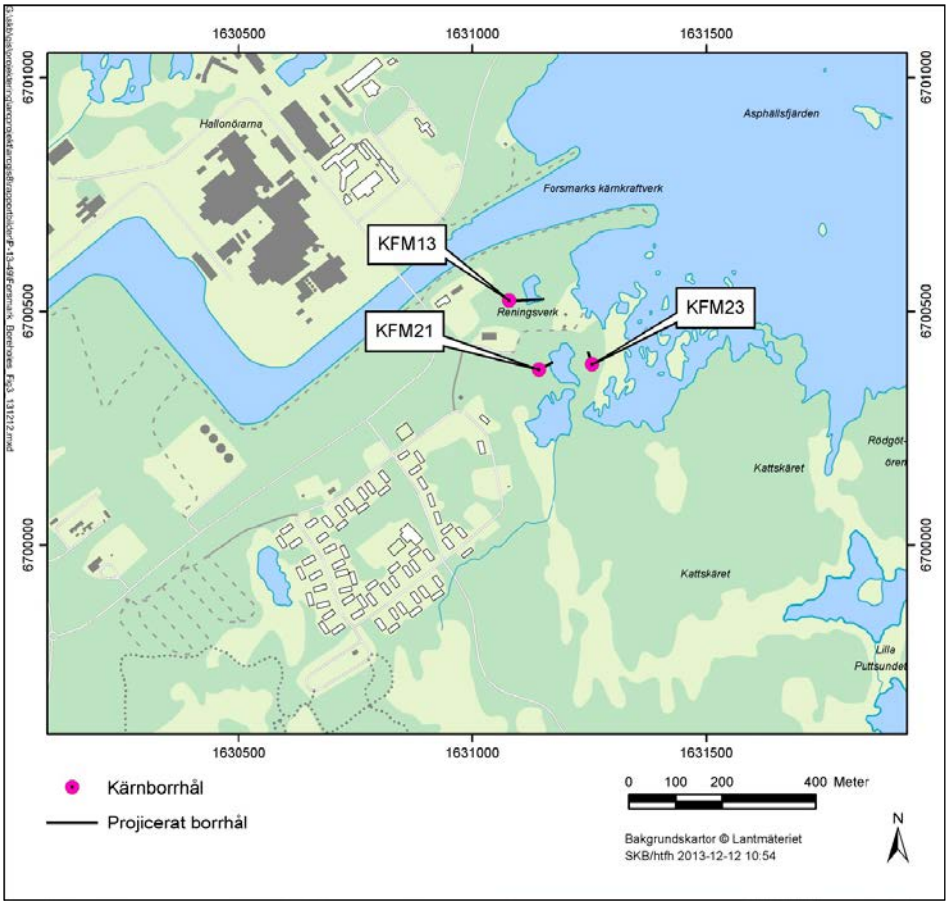

Figure 5-5. *Boreholes at the land site within the nuclear waste disposal area with boreholes KFM21, KFM13 and KFM23 marked. Also the vectors V3 and V4 are shown.*

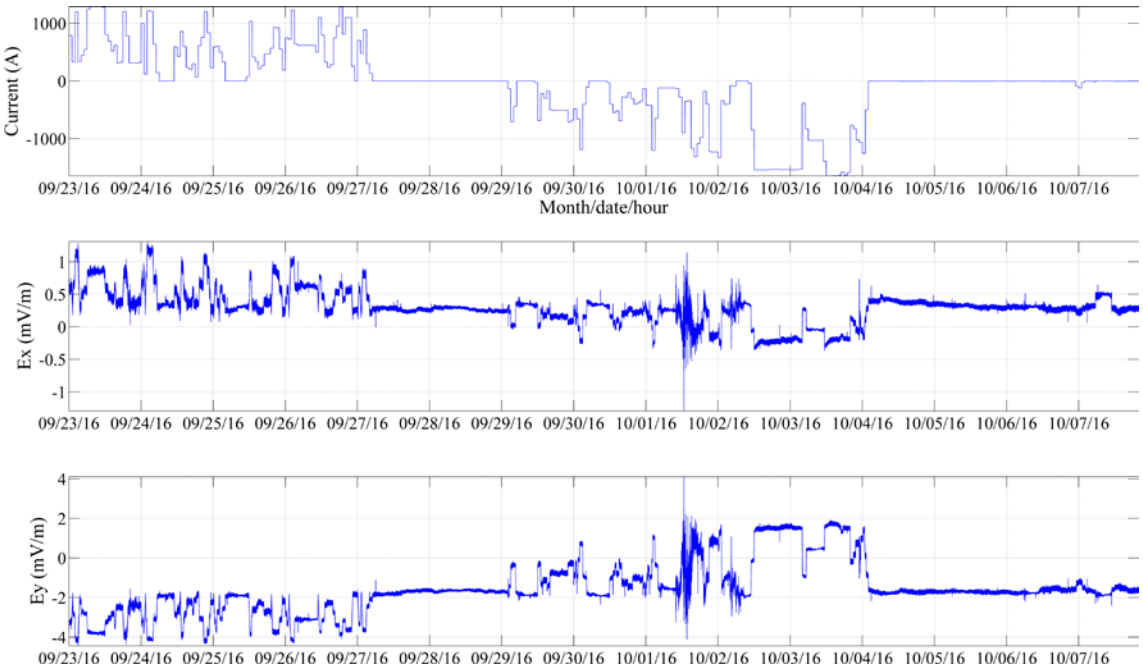

Figure 5-6. *Variation of the horizontal electric field at the land site, Forsmark, and current injected at Fågelsundet. Ex corresponds to V3 and Ey to V4.*

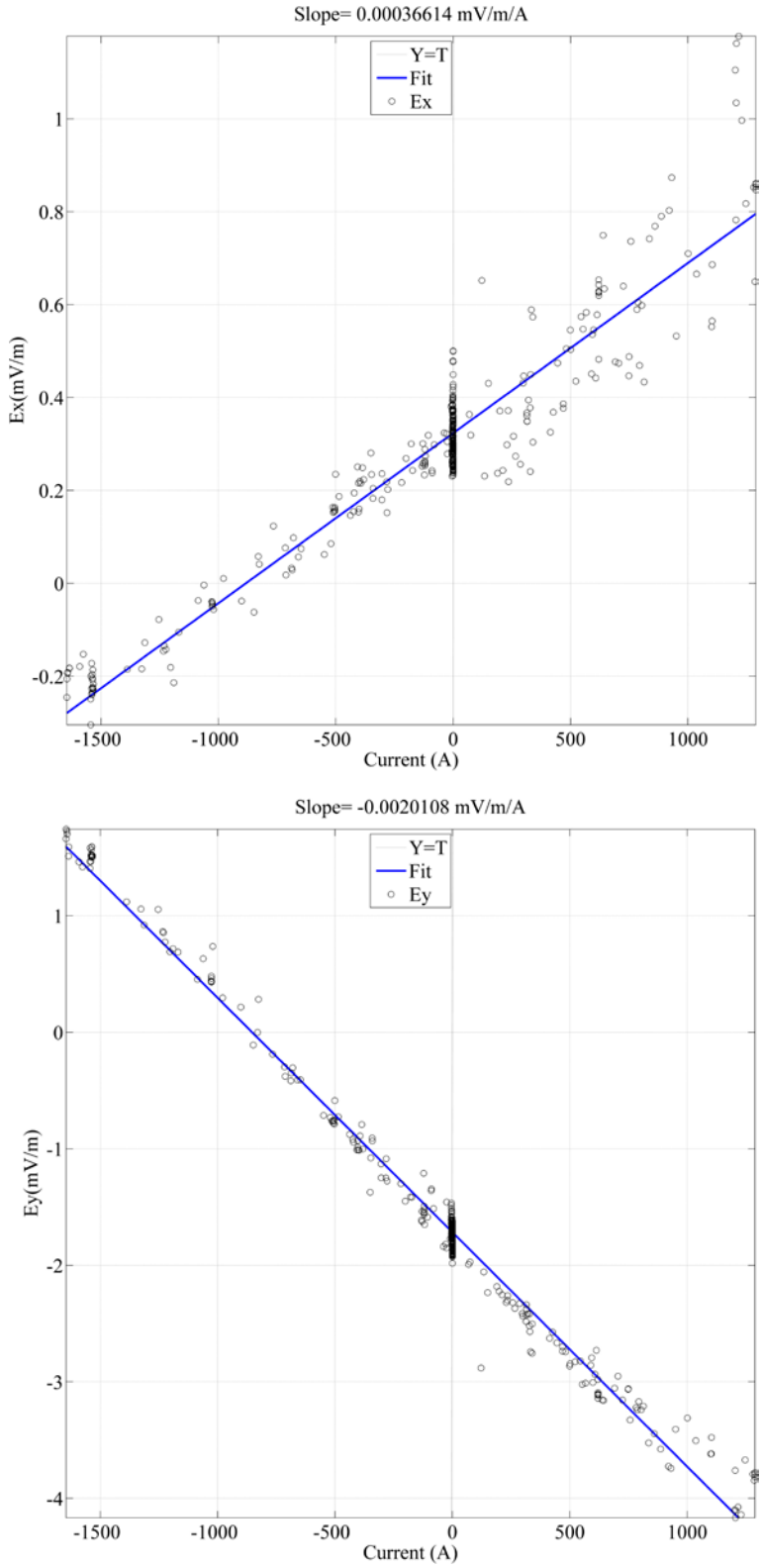

Figure 5-7. *Regression analysis of measured electric fields, Ex (V3) and Ey (V4) at land site.*

6 Summary and discussion

A summary of the results from the pier and the land sites are shown in Table 6-1.

The magnitude of the induced potential gradients from the injection point at Fågelsundet shows a rather large variation from the pier site to the land site and the direction of the maximum gradient differs considerably from the expected direction Forsmark to Fågelsundet that would be prevalent if the Earth's structure around Forsmark had been a simple horizontally layered one. However, lateral variations in the electrical conductivity due for example to vertical/near vertical fracture zones can distort the magnitude and direction of current flow and the corresponding changes in potential gradients. The distortions of the gradients can be particularly strong where the gradient in electrical conductivity is high, as will be the case when the fracture zones are saturated with saline fluids.

In spite of these complications, the average sensitivity of the potential gradients to the current injected at Fågelsundet can be assessed to be in the order of the magnitude 1 mV/m per 1,000 A.

Table 6-1. Sensitivity of electric field at Forsmark sites to current injection at Fågelsundet.

	Slope [mV/km/A]	Intercept [mV/km]	Remarks
Pier site			
V1	–0.25	70	
V2	+0.43	–60	
tangential	–0.32	60	Effective horizontal slope is 423 mV/km/kA.
normal	+0.27	60	Azimuth is 283°.
Land site			
V3	+0.37	+320	
V4	–2.01	–1,650	
tangential	–0.89	750	Effective horizontal slope is 2,040 mV/km/kA.
normal	+1.84	+1,600	Azimuth is 262.9°.

References

SKB's (Svensk Kärnbränslehantering AB) publications can be found at www.skb.se/publications.

Pedersen L B, Smirnov M, Kalscheuer T, Dynesius L, 2008. Measurements of Earth potentials at Forsmark. SKB P-08-19, Svensk Kärnbränslehantering AB.

Smirnov M, Korja T, Dynesius L, Pedersen L B, Laukkanen E, 2008. Broadband magnetotelluric instruments for near-surface and lithospheric studies of electrical conductivity: a Fennoscandian pool of magnetotelluric instruments. Geophysica 44, 31–44.

Appendix 1

Additional time series and regression plots for the pier site

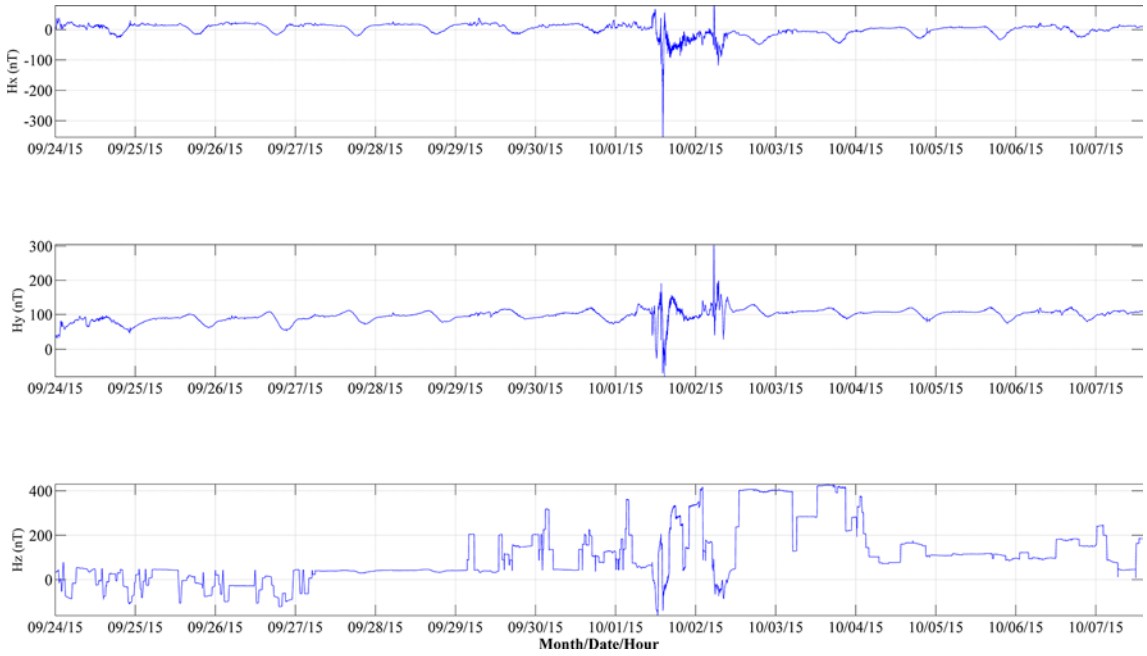

Figure A1-1. *Magnetic field components H_x, H_y and H_z, where x denotes Magnetic North, y Magnetic East and z downwards. Note that Hz is severely affected by the current injected at Fågelsundet. The reason is that the two cables in the Fenno-Skan system pass by the Forsmark sites at close distance. The distance to the two cables is slightly different whereby a minor difference in slopes can be expected for positive and negative currents. Note also that DC current in the cables has no effect on the electric field components.*

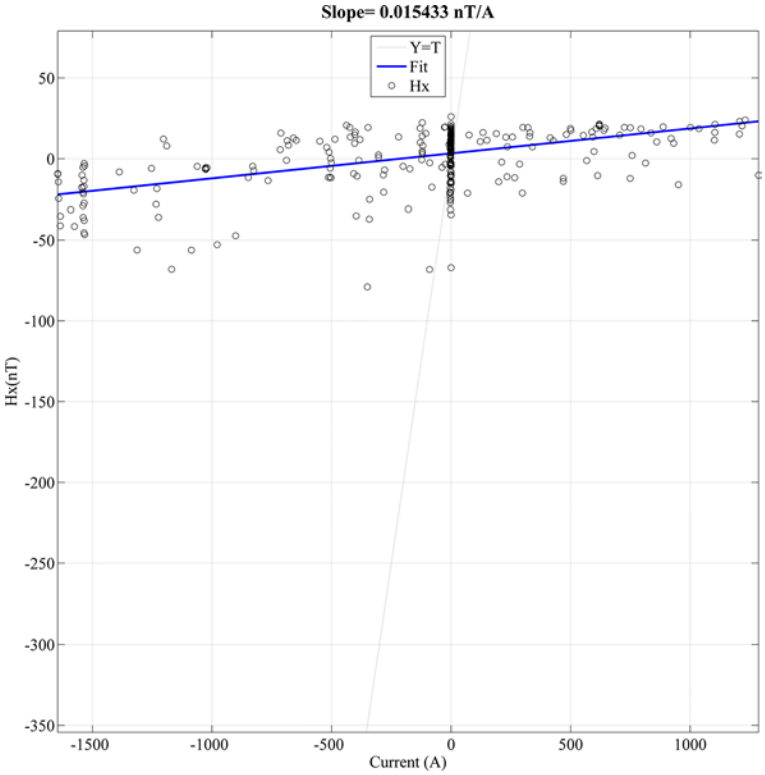
Slope= 0.015433 nT/A
Y=T
Fit
Hx
Hx(nT)
Current (A)

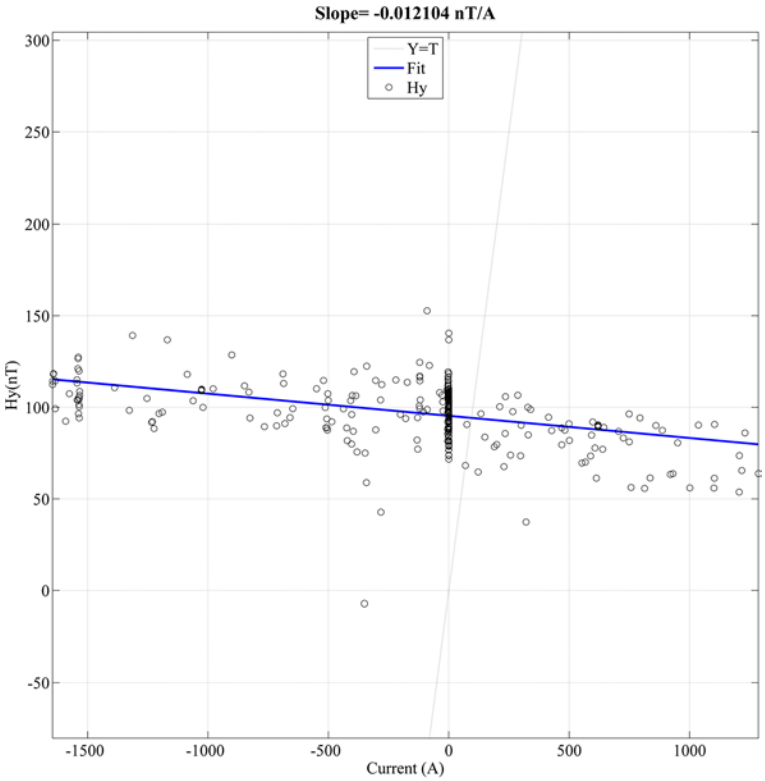
Slope= -0.012104 nT/A
Y=T
Fit
Hy
Hy(nT)
Current (A)

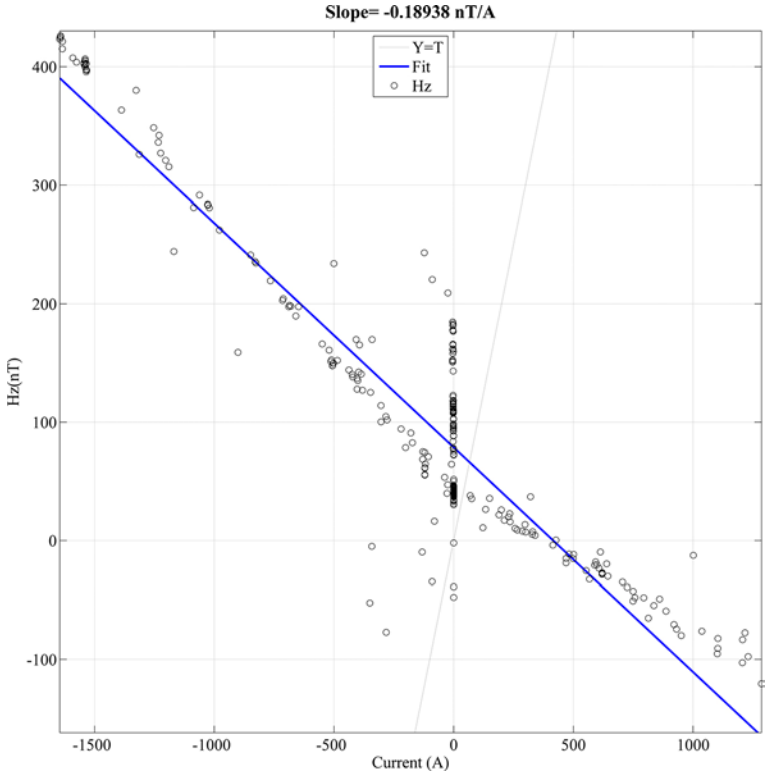

Figure A1-2. *Regression lines for the magnetic field components. Note that the effect on the horizontal magnetic field is negligible as expected for a nearby line current, whereas the vertical field is severely affected. Note also that the slopes for negative and positive currents for the vertical magnetic component are slightly different because the distance to the two cables in the Fenno-Skan system is different. The cable carrying the negative current lies closer to the observation point on the pier than the cable carrying the positive current, because the slope for negative currents is steeper than the slope for positive currents. The intercepts for zero currents differ from zero because the static magnetic field from the Earth's main field is not entirely compensated for. This has no effect on the slopes. The dashed Y=T is of no importance since it only shows the current as a function of current.*

Appendix 2

Additional time series and regression plots for the land site

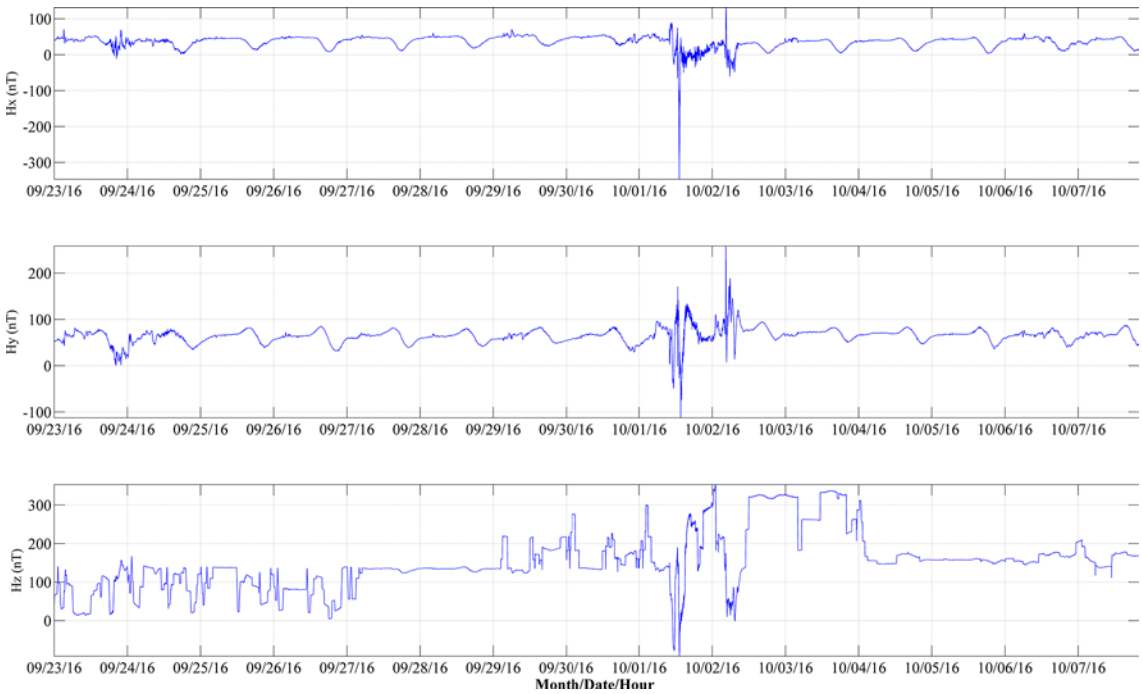

Figure A2-1. *Magnetic field components H_x, H_y and H_z, where x denotes Magnetic North, y Magnetic East and z downwards. Note that Hz is severely affected by the current injected at Fågelsundet. The reason is that the two cables in the Fenno-Skan system pass by the Forsmark sites at close distance. The distance to the two cables is slightly different whereby a minor difference in slopes can be expected for positive and negative currents. Note also that DC current in the cables has no effect on the electric field components.*

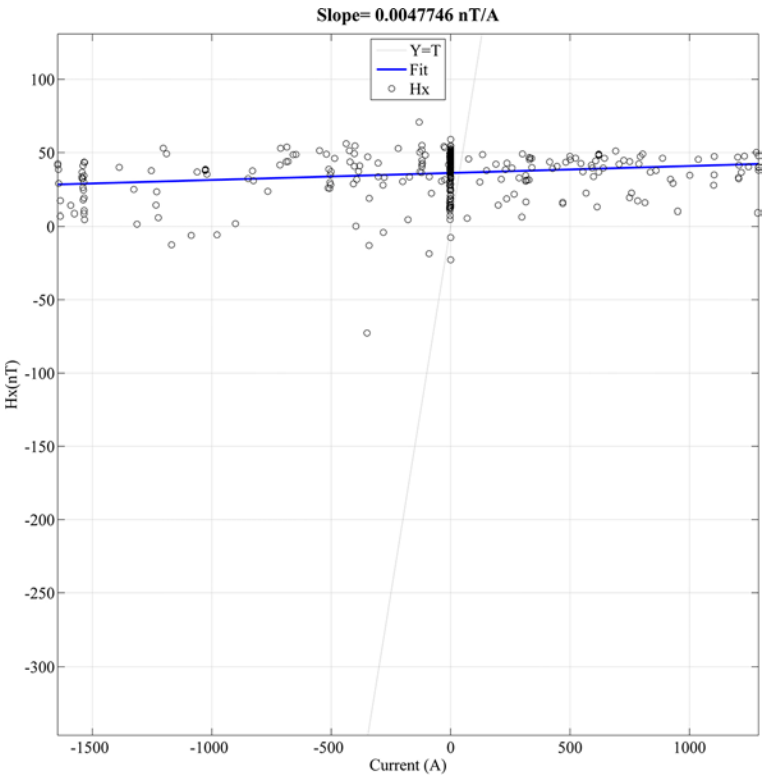
Slope= 0.0047746 nT/A
Y=T
Fit
Hx
Hx(nT)
Current (A)

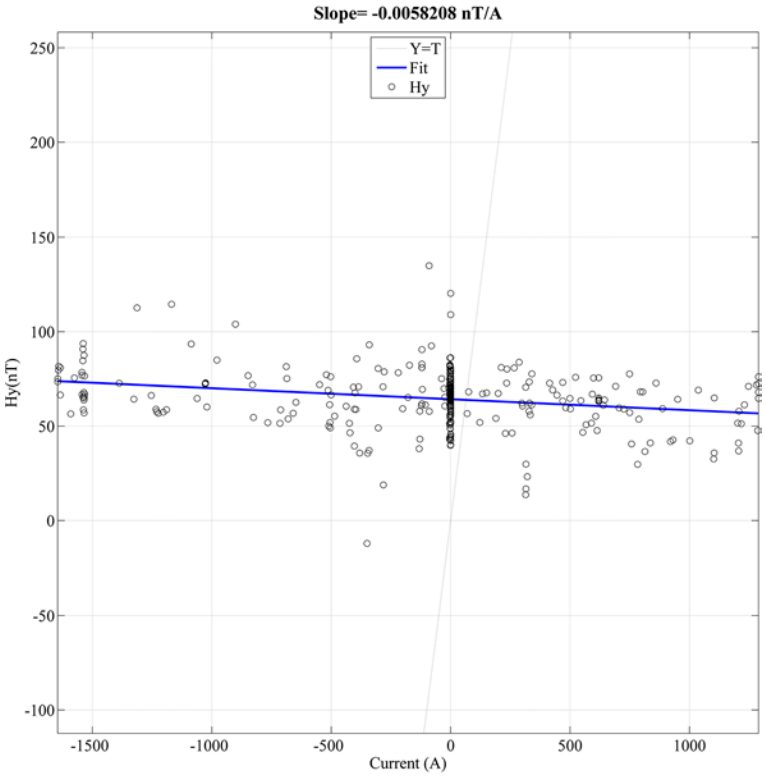
Slope= -0.0058208 nT/A
Y=T
Fit
Hy
Hy(nT)
Current (A)

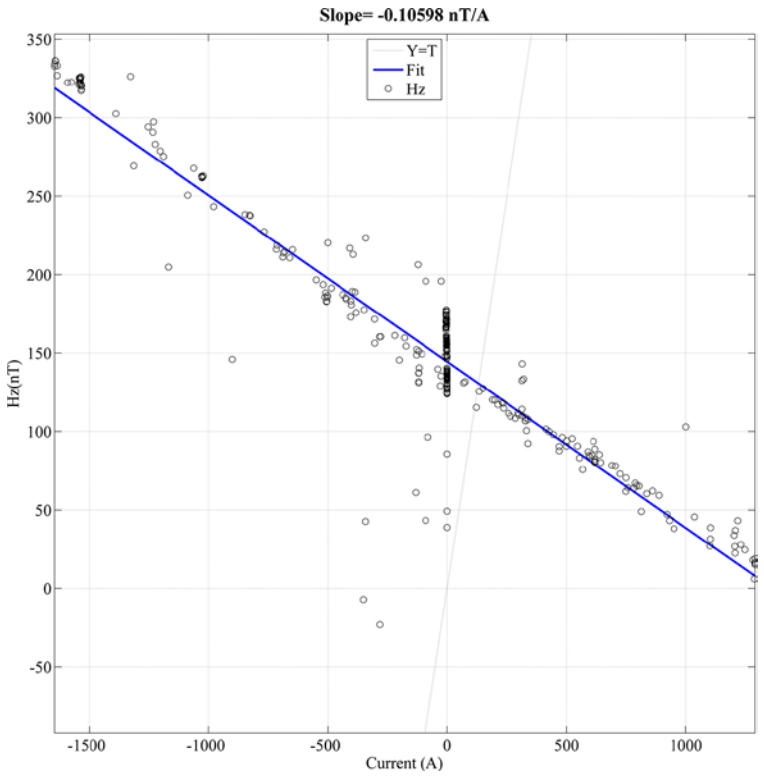

Figure A2-2. *Regression lines for the magnetic field components. Note that the effect on the horizontal magnetic field is negligible as expected for a nearby line current, whereas the vertical field is severely affected. Note also that the slopes for negative and positive currents for the vertical magnetic component are slightly different because the distance to the two cables in the Fenno-Skan system is different. The cable carrying the negative current lies closer to the observation point on the pier than the cable carrying the positive current, because the slope for negative currents is steeper than the slope for positive currents. The intercepts for zero currents differ from zero because the static magnetic field from the Earth's main field is not entirely compensated for. This has no effect on the slopes. The dashed Y=T is of no importance since it only shows the current as a function of current.*

Appendix 3

Calculating the electric field from measurements in a skewed coordinate sytem.

Defining angles θ_1 and θ_2 for the measured components v_1 and v_2, the direction cosines of their normals n_1 and n_2 can be expressed as $(-\sin\theta_1\,,\ \cos\theta_1)$ and $(-\sin\theta_2\,,\ \cos\theta_2)$, respectively.

Angles θ_t and θ_n for the components t and n define their direction cosines as

$$\hat{t} = (\cos\theta_t, \sin\theta_t) \qquad \text{(A3-1a)}$$

and

$$\hat{n} = (\cos\theta_n, \sin\theta_n), \qquad \text{(A3-1b)}$$

respectively.

All angles are defined in the x-y coordinate systems and counted clockwise from N towards E. The total vector, v, is found from the point where the lines n_1 and n_2 cross each other. Having found v, the components t and n are found by projecting v onto the unit vectors along t and n.

Mathematically we then have:
the lines along n_1 and n_2 have parametric representations given by

$$v_1(\cos\theta_1, \sin\theta_1) + (-\sin\theta_1\,,\ \cos\theta_1)\,t_1 \qquad \text{(A3-2a)}$$

and

$$v_2(\cos\theta_2, \sin\theta_2) + (-\sin\theta_2\,,\ \cos\theta_2)\,t_2 \qquad \text{(A3-2b)}$$

where t_1 and t_2 vary from minus to plus infinity.
At the cross point between the lines the x- and y-components are equal, and we can write

$$v_1(\cos\theta_1, \sin\theta_1) + (-\sin\theta_1\,,\ \cos\theta_1)\,t_1 = v_2(\cos\theta_2, \sin\theta_2) + (-\sin\theta_2\,,\ \cos\theta_2)\,t_2$$

or written for each component

$$v_1\cos\theta_1 - \sin\theta_1\,t_1 = v_2\cos\theta_2 - \sin\theta_2\,t_2 \qquad \text{(A3-3a)}$$

$$v_1\sin\theta_1 + \cos\theta_1\,t_1 = v_2\sin\theta_2 + \cos\theta_2\,t_2 \qquad \text{(A3-3b)}$$

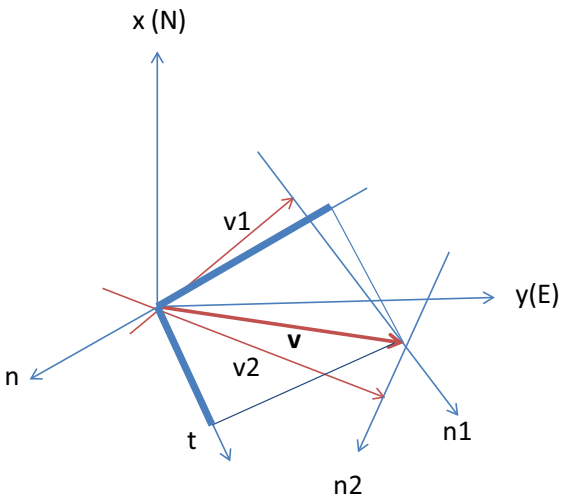

Figure A3-1. *Measured E-field components v_1 and v_2 with normals n_1 and n_2. Crosspoint of normals defines the total electric field vector v. Vector v is decomposed into tangential and normal components along unit vectors $\hat{\boldsymbol{t}}$ and $\hat{\boldsymbol{n}}$, respectively. Azimuths of vectors not shown.*

Eliminating the unknown t_1 we obtain a simple linear equation for t_2

$a = b + ct_2$

where

$a = v_1 \tan \theta_1 + \text{cotan } \theta_1$

$b = v_2 \dfrac{\cos \theta_2}{\sin \theta_1} + \dfrac{\cos \theta_2}{\cos \theta_1}$

$c = \dfrac{\cos \theta_2}{\cos \theta_1} - \dfrac{\sin \theta_2}{\sin \theta_1}$

so that the cross point is defined by

$$v = (v_x, v_y) = v_2 (\cos \theta_2, \sin \theta_2) + (-\sin \theta_2 , \cos \theta_2)\, t_2 \qquad \text{(A3-4)}$$

Finally v is projected onto the t- and n-axes by

$$v_t = \hat{t} \cdot v \qquad \text{(A3-5a)}$$

and

$$v_n = \hat{n} \cdot v. \qquad \text{(A3-5b)}$$